Extrapolation of extreme traffic load effects on a cable-stayed bridge based on weigh-in-motion measurements

Naiwei Lu *

School of Civil Engineering,
Changsha University of Science and Technology,
Changsha Hunan 410114, China
Email: lunaiweide@163.com

Yang Liu

School of Civil Engineering,
Changsha University of Science and Technology,
Changsha Hunan 410114, China
Email: liuyangbridge@163.com

Michael Beer

Institute for Risk and Reliability,
Leibniz Universität Hannover,
Hannover 31509, Germany
and
Institute for Risk and Uncertainty,
University of Liverpool,
Liverpool 69 3BX, U.K.
and
International Joint Research Center for Engineering Reliability and Stochastic Mechanics,
Tongji University
Shanghai 200092, China
Email: beer@irz.uni-hannover.de

Abstract: The steadily growing traffic loading may become a hazard for the bridge safety. Compared to short and medium span bridges, long-span bridges suffer from simultaneous presence of multiple vehicle loads. This study presents an approach for extrapolating probabilistic extreme effects on long-span bridges based on weigh-in-motion (WIM) measurements. Three types of stochastic traffic load models are simulated based on the WIM measurements of a highway in China. The level-crossing rate of each stochastic traffic load is evaluated and integrated for extrapolating extreme traffic load effects. The probability of exceedance of a cable-stayed bridge is evaluated considering a linear traffic growth model. The numerical results show that the superposition of crossing rates is effective and feasible to model the probabilistic extreme effects of long-span bridges under the actual traffic loads. The increase of dense traffic flows is sensitive to the maximum load effect extrapolation. The dense traffic flow governs the limit state of traffic load on long-span bridges.

Keywords: bridge; traffic load; extreme value; level-crossing theory; weigh-in-motion; probability of exceedance

1 Introduction

A large number of highway bridges were built over the past decades under the guidelines of national design specifications. The live load specified in the national design specification is conventionally evaluated based on site-specific traffic measurements collected several decades ago. For instance, the live load in the Load and Resistance Factor Design code of America (AASHTO, 2007) was evaluated based on data collected in Ontario in the 1970s (Nowak 1994). The live load in Eurocode 3 (ECS 2005) was made based on weeks of data collected in Auxerre in the 1980s. The China's code (MOCAT 2015) was made based on five highway traffic measurements in the 1990s. However, the current traffic load has increased significantly, which may become a hazard for serviceability, fatigue or even safety of existing bridges (Fu and You 2009). In fact, several short and medium span bridges collapsed due to extremely overloaded trucks. Han et al. (2014) indicated that 4 out of 1319 trucks in China cause larger bending moments of short-span bridges than the one evaluated according to the national design specification. Long-span bridges suffer from the simultaneous presence of multiple vehicle loads compared to short-to-medium span bridges (Chen and Wu 2010). Therefore, evaluation of maximum traffic load effects on long-span bridges using actual traffic data deserves investigation.

Traffic measurements are essential for modelling actual traffic load models, because traffic loads on a bridge are random and site-specific in nature. With developments of weight-in-motion (WIM) technologies (Yu et al. 2016), a traffic database is available for simulating and predicting multi-objective traffic load models. In this regard, Miao and Chen (2002) utilized WIM data in Hong Kong to develop a truck load model and compared it to several existing bridge live-load models. The WIM measurements in Netherlands were utilized by Oconnor and Obrien (2005) to extrapolate the maximum traffic load effect of a short-span bridge. A great number of WIM records collected from five European sites with consideration of overloaded or over-length vehicles were utilized by OBrien and Enright (2012) to simulate the maximum effect of short-to-medium span bridges under free-flowing traffic loads. Zhang and Au (2016) utilized WIM measurements in China to evaluate fatigue reliability of a long-span bridge. These studies have made great contribution to traffic load simulation based on WIM measurements. Lu et al. (2017b) evaluated the maximum deflection of a suspension bridge considering traffic volume growth based on WIM data in China. The traffic density variation that is a common phenomenon on highways has a significant influence on the load effects of long-span bridges. However, the traffic density has been ignored in the existing traffic load models.

Investigation on effective approaches for probabilistic extrapolation of traffic load effects on bridges is a hot research field. The conventional approaches are the peaks over threshold (PVT) approach, generalized extreme value (GEV) distribution, and Rice level-crossing theory (OBrien et al., 2014; Zhou et al., 2016). The block maxima load effects for short and medium span bridges have a better fitting by the GEV distribution (Enringt and OBrien, 2013). However, the Rice's level-crossing theory has advantages in probabilistic extrapolation of the traffic load effects on long-span bridges that can be assumed stationary and Gaussian (Cremona, 2001). For the Rice theory, the premise is the Gaussian process, and the key problem is how to determine the optimum interval to fit the crossing rate. This problem has been discussed by many researchers (O'Brien et al. 2015; Chen et al., 2015). On the basis of extrapolations, the characteristic load effect can be estimated for bridge design considering a lifetime return period.

As elaborated above, the site-specific traffic measurements provide a huge database for the modelling the live load of in-service bridges. In addition, the stochastic traffic flow is an effective and realistic model that needs to be considered especially for long-span bridges due to the severe vibration in contrast to the transient vibration caused by a single vehicle on a short span bridge. To the best of the authors' knowledge, most studies on this field focused on maximum traffic load effects analysis of short to medium span bridges. However, research efforts on long-span bridges are relatively insufficient. In practice, due to the statistical parameters in the stochastic flow model, the corresponding load effects can be further developed for application of probabilistic modelling such as extrapolation of extreme values and reliability assessments. One of the difficulties in this regard is the time-consuming traffic load effect analysis. Moreover, probabilistic modeling of load effects requires additional long-term traffic loads database.

This study aims to implement Rice's level-crossing theory to extrapolate the probabilistic extreme effects on long-span bridges under site-specific traffic loads. The WIM measurements of a heavy-duty highway in China are utilized to simulate the interval-density stochastic traffic-load models. The level-crossing rate for the variable-density traffic is integrated by the level-crossing rates of three interval-density traffics. Characteristic deflections and probability of exceedance of a cable-stayed bridge are evaluated with consideration of a linear traffic growth model. The effective and feasible of the proposed framework is demonstrated in a case study of a cable-stayed bridge.

2 Theoretical bases

Similar to the generalized extreme value distributions, Rice's level-crossing theory is an effective approach to predict maximum traffic load effect on long-span bridges in a reference period. The premise of utilizing the level-crossing formula is to presume the stationarity of a stochastic process. However, due to the variable density of the actual traffic flow on a long-span bridge, the traffic load effect is obviously non-stationary, which violates the premise of the Rice's theory. Therefore, this study utilizes an effective approach to consider the variable-density traffic loads.

2.1 Rice's level-crossing formula

For long-span bridges, the ratio between the bridge length and the consecutive vehicle spacing is larger than that of short and medium span bridges. Therefore, the load effects of long-span bridges under stable traffic loads can be assumed stationary and Gaussian, or even be modelled as white noise processes (Ditlevson 1994). Rice's level-crossing theory (see Fig. 1) is a conventional approach to deal with a stationary stochastic process exceeding a threshold level during a reference period. Level-crossing rate that is the number of crossings in a unit period can be written as (Rice 1945):

$$v(x) = \frac{\sigma^{'}}{2\pi\sigma}\exp\left[-\frac{(x-m)^2}{2\sigma^2}\right] \tag{1}$$

where, x is a threshold level, m and σ are the mean value and standard deviation of the random process, respectively, and σ' is the standard deviation of the derivative of x. In practice, $v(x)$ can be fitted to histograms of number of crossings in a unit time. In particular to traffic load effects on bridges, $v(x)$ can be approximated by the numerical simulations with traffic data and structural influence lines.

The critical step for extrapolating is to choose the optimal starting point and number of intervals. A starting point close to the tail is better for the approximated to the tail, while a starting point far from the tail is better for the extrapolation. In this regard, Cremona (2001) suggested a Kolmogorov-Smirnov test to optimize the starting point. In order to deal with the subjective of the significance level in the Cremona's approach, Chen et al. (2015) developed the Rice's method by utilizing empirical distribution of random variables. Based on the optimal starting point and class intervals, the maximum value in a return period is written as (Cremona 2001)

$$x_{\max}(R_t) = m_{opt} + \sigma_{opt}\sqrt{2\ln(v_{0,opt}R_t)} \tag{2}$$

where, R_t is the return period, $x_{\max}$ is the maximum load effect corresponding to the return period, m_{opt}, σ_{opt} and $v_{0,\mathrm{opt}}$, represent the optimal mean value, optimal standard derivation and optimal crossing rate, respectively. It is worth to note that the plus sign in the second part of Eq. (2) can be changed to the minus sign to evaluate the minimum extrapolation.

Based on the relationship of the return period and the reference period, the cumulative distribution function (CDF) of the maximum traffic load effect during the lifetime of a bridge can be written as

$$F_{\max}(x) = \exp\left[-T_{ref}v_{0,\mathrm{opt}}\exp\left(-\frac{1}{2}\left(\frac{x-m_{opt}}{\sigma_{opt}}\right)^2\right)\right] \tag{3}$$

where, T_{ref} is the reference period. It is obvious that the CDF is a variation of Gumbel distribution where the kernel part is $\frac{1}{2}(\frac{x-m_{opt}}{\sigma_{opt}})^2 - \ln(v_{0,opt}T_{ref})$.

2.2 Bridge level-crossing rates under actual traffic loads

The premise of utilizing the Rice's formula is to ensure the stationary of the stochastic process. It is acknowledged that the traffic flows on bridges are time varying, where the traffic is dense at daytime and is free at night. Therefore, the traffic load on a long-span bridge will cannot be traded as stationary during the service period. However, the traffic load can be assumed as stationary in an interval time that can be evaluated from the traffic density distribution in one day. For instance, based on the WIM data of a highway bridge in Sichuan, China, the hourly traffic volume in two lanes was evaluated as shown in Fig. 2. The dash lines of 200 and 400 vehicles per hour divide the entire traffic flow into three parts, including the dense traffic flow, the moderate traffic flow and the sparse traffic flow. The expected numbers of vehicles are 8.3, 5.0 and 1.7 per hour per lane for the three types of traffic flows, respectively.

By dividing the entire nonstationary process into several stationary interval processes, the level-crossing rate of the original process can be treated as a superposition of the interval processes in proportions. Based on this assumption, the kernel coefficients can be evaluated by a second-order polynomial function:

$$\ln\left[\overline{v}(x)\right] = \ln\left[\sum_{i=1}^{m} \frac{p_i N_i(x)}{T}\right] = a_0 + a_1 x + a_2 x^2 \tag{4}$$

where, $\overline{v}(x)$ is a estimated equivalent level-crossing rate of the non-stationary process, $a_0 = \ln(v_0) - \frac{m^2}{2\sigma^2}$, $a_1 = \frac{m}{\sigma^2}$, and $a_2 = \frac{1}{-2\sigma^2}$ are second-order polynomial coefficients that can be evaluated based on the histograms of number of crossings. Subsequently, the maximum value during a return period can be estimated as shown in Eq. (3). In this way, the non-stationary process problem has been solved by utilizing an interval stationary process. The probability distribution of the vehicle spacing can be estimated from the WIM records in each time interval.

In addition to the maximum value extrapolation based on the level-crossing formula, probability of exceedance can also be estimated. First-passage failure is the best description of stochastic process crossing the prescribed threshold during an interval time. Based on the Rice's level-crossing theory, the probability of failure, P_f, can be estimated by the assumption of a Poisson distribution:

$$P_f(a, T_s) = A\exp\left[-\int_0^{T_s} v_i(a)\,\mathrm{d}\,t\right] \cong \exp\left[-T_s \overline{v}(a)\right] \tag{5}$$

where, A is a coefficient associated with the stationarity of a random process and can be assumpted as 1 for a stationary process, T_s is usually the lifetime of a bridge, and a is the threshold value of the bridge, such as L/500 for the deflection limit of a concrete cable-stayed bridge (MOCAT 2007).

3 Methodology of level-crossing rate simulation of long-span bridges under variable-density stochastic traffic loads

Fitting level-crossing rates is a critical step to implement the Rice's theory to evaluate the maximum traffic load effect on a bridge. In general, the level-crossing rate can be fitted to the block maxima via MCS, which is applicable for short and medium span bridges.

However, long-span bridges suffer from simultaneous vehicle loads that lead to the complexity of the block maxima simulation. Moreover, the variable-density characteristic of the traffic loads on long-span bridges results in the nonstationarity of the live-load effects, which violate the premise of the Rice's formula. As an extended application of the interval level-crossing model, a framework is present in the present study to simulate the level-crossing rate of long-span bridges under actual stochastic traffic loads.

The flowchart of the proposed computational framework is shown in Fig. 3. The initial task as depicted in the flowchart is to simulate several interval stochastic traffic flows based on the WIM measurements. The statistical analyses of the filtered WIM measurements are conducted to obtain the probability models that are essential for stochastic traffic load simulation. According to the predefined traffic density threshold as shown in Fig. 2, divide the daily traffic flow into several types of interval traffics. The probability density functions (PDFs) of the vehicle spacing are fitted to the histograms of the interval traffics. Eventually, the interval stochastic traffic load models can be simulated based on the PDF models of traffic flows via the MCS. The actual traffic flow can be deemed as the integration of the interval traffic flows in proportions.

Based on the simulated interval stochastic traffic loads, the load effects can be evaluated by the bridge static influence lines. The static response rather than the dynamic response are considered for long-span bridges because the dynamic amplification factor for flexible long-span bridges are less than 1.05 as specified in many design codes. The number of crossings as described in Fig. 1 can be counted as histograms where the level-crossing rate can be fitted via a polynomial function as shown in Eq. (4). An equivalent level-crossing rate for the actual traffic flow can be approximated to the superposition of the interval level-crossing rates in proportions. With the equivalent level-crossing model, predications of the maximum load effect and the probability of failure can be conducted based on Eq. (2) and Eq. (5). It is worth to note that this framework can also be implemented to investigate the influence of traffic change in proportions of the interval traffic flows on the maximum load effect extrapolation and the probability of failure.

The efficiency and accuracy of the computational framework mostly depend on the number of the interval traffic flows. For instance, the actual traffic in the present study is divided into three parts as shown in Fig. 2. Obviously, traffic load models with a shorter interval density length leads to a more accurate approximation to the actual traffic. Since the bridge static influence line is utilized to estimate the traffic load effect, the computational effort is negligible.

4 Level-crossing rate simulation of a cable-stayed bridge

A long-span cable-stayed bridge and its WIM measurements are selected herein to demonstrate the application of the proposed approach. The influence of the traffic density on the level-crossing rate is investigated.

4.1 Stochastic traffic load simulation based on WIM measurements

The WIM measurements in the present study were collected from a heavy-duty highway bridge in Sichuan, China. Details of the WIM measurements can be found in Liu et al. (2015) and Lu *et al.* (2017a). Since the original data contains some error and invalid data that is useless for the present study, a filtering process was conducted to remove these invalid data. In addition, the highly occupied light cars have slight contribution to the traffic load effect, and thus should be removed. According to the suggestion given by

Enright and Obrien (2013), the present study utilized the following criteria to filter the invalid data: (1) the GVW was less than 30 kN; (2) the axle weight was greater than 300 kN or less than 5 kN; and (3) the vehicle length was more than 20 m. The overview of the effective measurement is shown in Table 1. According to the vehicle configuration, all vehicles were classified as 6 types, where V1 represents light cars, V2~V6 represent the 2- to 6-axle trucks.

The essential statistics of the traffic flows are shown in Figs. 4. In Fig. 4(a), the GVW of the 6-axle trucks is well fitted by a bimodal Gaussian mixture model (GMM), where w_i, μ_i and σ_i are parameters in the Gaussian distribution. It is worth to note that the second peak of the probability model of the GVW resulting from the overloaded trucks is well captured by the GMM model. In Fig. 4(b), x_i and p_i are the vehicle spacing and proportion of the ith type of traffic flows as defined in Fig. 2. The probability models of the vehicle spacing of various traffic densities were modelled separately by lognormal distribution functions.

Based on the statistics of WIM measurements, the conventional MCS approach (Caprani et al. 2008; Enright Obrien 2013) was utilized to simulate the stochastic traffic load model. The first step is to determine the type of a vehicle according to the uniformly distributed PDF of the vehicle type proportion. The second step is to sample the GVW of the vehicle and the driving lane according to the statistics of the type of vehicles. The final step is to determine the vehicle spacing between two vehicles in the same traffic lane. The advantage for the segmental stochastic traffic load model is the feasibility of converting of the nonstationary daily traffic load into segmental stationary processes.

4.2 Deflection-time history simulation of a cable-stayed bridge

Dimensions of the prototype long-span cable-stayed bridge are shown in Fig. 5. The bridge has two pylons with double-sided cables following a fan pattern. The pylon and segmental girders are connected by 34 pairs of cables in double sides. The length and height of each steel box-girder are 12.8 m and 3 m, respectively. There are 4 traffic lanes in opposite directions.

A commercial program ANSYS was used to extract the static deflection influence lines from the finite element model of the bridge. In the finite element model as shown in Fig. 6, the beams and towers were simulated by beam elements, and the cables were simulated by link elements. The cable forces are considered by the initial strain. The modulus of elasticity of the cables was revised based on the Ernst’s equation (Freire et al. 2006):

$$E_{eq} = E\frac{1}{1+\dfrac{q^2L_h^2}{12T^3}EA} \tag{6}$$

where, E is the Young modulus of the material, T is the cable force, q is the unit self-weight per length, L_h is the horizontal length of the cable, A is the cross-sectional area. A unit force was considered to move through the bridge, and the deflection influence lines at the points L/4, L/2 and 3L/4 are plotted in Fig. 7. It is observed that the critical point is the mid-span (L/2) point. Therefore, the subsequent analysis focuses on the mid-span point of the bridge girder.

Based on the influence lines, the deflection-time histories of the bridge under the simulated stochastic traffic loads were calculated. The moving step of the traffic flow on the bridge is 6 m that is the cable spacing on girders. The computational effort is ignorable for the static analysis. One of the daily deflection-time histories is shown in Fig. 8, where $D_{\max}$ is the maximum deflection for a type of traffic loads in one day.

It is obvious that the dense traffic load leads to more higher extreme values compared to the free traffic load. In addition, the three types of time-histories can be distinguished easily by the extreme values. This phenomenon explains the necessary of dividing the variable-density daily traffic flow into several intervals of constant-density traffic flows. In this way, the bridge deflections have been divided into three types of stationary deflections.

4.3 Deflection crossing rate simulation

Based on the daily deflection histories of each interval traffic loads, the number of level-crossings can be counted and the crossing rate can be fitted by lognormal functions and polynomial functions. In order to make a more accurate extrapolation based on the level-crossing model, 1,000-day traffic flows were simulated where 30% upper data were utilized to approximate the annual deflection crossing rate. The effects of the three types of traffic flows were simulated and analysed separately, and the histograms of the actual traffic loads were accumulated considering the proportions of the three traffic flows. Fig. 9 plots the individual histograms and corresponding fittings. Parameters of the fitting are shown in Table 2.

In Fig. 9, each type of histogram corresponds to a type of traffic loads. The line for the actual traffic loads is a mixture of the three level-crossing rates. It is obvious that the actual traffic model has taken into account different types of traffic loads. In addition, influence of each type of traffic flows on the actual level-crossing model can be investigated by changing their proportions. Therefore, the proportions of the traffic flows were doubled respectively to investigate their influence on the actual level-crossing rate. It is observed from Fig. 10 that the dense traffic flow impacts the tail of the fitting for the actual traffic load.

Herein, the deflection crossing models of the cable-stayed bridge are simulated based on the WIM measurements. The nonstationary of the traffic loads have been solved by dividing the daily traffic flow into three intervals of constant-density traffic flows. Since the tail of the level-crossing rate fitting is mostly impacted by the dense traffic loads, numerical study of its influence on the probability of exceedance of the bridge limit is investigated.

5 Probabilistic extreme traffic load effects

Based on the estimated level-crossing model, the characteristic traffic load effects and the probability of exceedance are evaluated with the consideration of the traffic density.

5.1 Maximum deflection extrapolation

The purpose of the level-crossing rate fitting is to extrapolate the maximum traffic load effect of a bridge in a reference period. Based on the level-crossing model, the maximum deflection of the bridge in a 1000-year lifetime was evaluated as shown in Fig. 11. In a 1000-year return period, the maximum deflections of the bridge under sparse, moderate and dense traffic loads are 0.493m, 0.541 m, and 0.721 m respectively. The maximum deflection for the actual traffic load is 0.703 that is relatively close to the one of the dense traffic load.

Since three traffic load models were utilized to superpose the level-crossing model, the influence of their proportions on the maximum deflection extrapolations is deserved investigating. Suppose two of the traffic proportions are constant, and change the third traffic proportion from 0 to 1. Fig. 12 plots the results, where the 100% dense traffic and the 100% sparse traffic load effects are included for comparison. As observed from Fig. 12, the maximum deflection value increase dramatically as the dense traffic appears, while the maximum deflection values increase slightly due to the proportion growth of the spare traffic and the moderate traffic. This phenomenon demonstrates that the proportion of the influence is the most sensitive factor leading to the maximum deflection.

5.2 Probability of exceedance assessment

As mentioned before, different design codes have different threshold values, such as L/300 and L/800. In the present study, the threshold deflection value is L/500=0.84 m according to MOCAT (2007) for long-span concrete cable-stayed bridges. It is defined as an event of exceedance that the bridge deflection crossing the threshold value in a 100-year period. Therefore, the probability of failure can be estimated based on the CDF of the level-crossing model. It is observed from Fig. 13 that the probabilities of failure are 7.9×10^{-6} and 8.2×10^{-5} for the current traffic loads and the double dense traffic loads, respectively. This result is analysed based on the assumption of stationary traffic loads. The double dense traffic means the traffic volume increase without reducing the vehicle spacing, because a variation of the distribution of the vehicle spacing results in the nonstationary of the traffic density.

In order to investigate the influence of density growth of the dense traffic on the probability of exceedance, the initial vehicle spacing in the stochastic traffic load model was supposed to be shortened by a reduction coefficient descripting the growth factor of the traffic. For instance, a reduction coefficient of a means the traffic volume grows by 1-1/(1-a). By re-evaluating the level-crossing rates and the superposition, the probability of the exceedance are plotted in Fig. 14. It is observed that a reduction coefficient of 0.54 corresponding to the traffic growth ratio of 117% is the threshold for a given probability of exceedance of 0.1 in a 100-year lifetime.

It can be concluded from the case study that the superposition of the level-crossing model simulated by interval stochastic traffic loads is an effective approach to predict the probabilistic extreme traffic load effects. Moreover, the influence of the different traffic proportions on the maximum deflection and the probability of exceedance can be analysed by utilizing the superposition of the level-crossing models.

6 Conclusions

This study presents a framework for probabilistic extrapolation of traffic load effects on long-span bridges based on WIM measurements. Three types of stochastic traffic load models are simulated based on the statistics of the WIM measurements of a heavy-duty highway bridge. Rice's level-crossing theory is implemented to approximate extreme traffic load effects. The actual crossing rate is integrated by the interval crossing rates of three types of traffic flows. Characteristic deflections and the probability of exceedance of a cable-stayed bridge are evaluated with consideration of a linear traffic growth model. The case study of the maximum deflection extrapolation of a cable-stayed shows the application of the framework in predicting probabilistic extreme traffic load effects. The dense traffic flow governs the limit state of traffic load on long-span bridges. The appearance of the dense traffic results in a dramatic increase of the maximum value extrapolation. A threshold traffic growth ratio can be evaluated based on the numerical result.

In addition to the cable-stayed bridges, the proposed approach can also be applied to any other flexible long-span bridges. However, some challenges need to be addressed in future works. First, since the dense traffic governs the extreme traffic loading scenario, a more detailed probability model focusing on the dense traffic is expected to provide a more reasonable extrapolation. Second, the congestion state rather than the free flowing state needs to be considered for the traffic load modelling. Finally, the nonlinearity of the traffic load effects can be considered by screening critical stochastic traffic loading scenarios based on influence lines.

References

American Association of State Highway and Transportation Officials (AASHTO). (2007). '*AASHTO LRFD Bridge Design Specifications*', Washington DC, USA.

Caprani, C.C., OBrien, E.J. and McLachlan, G.J. (2008) 'Characteristic traffic load effects from a mixture of loading events on short to medium span bridges', *Structural Safety*, Vol. 30, No. 5, pp. 394-404.

Chen, S.R. and Wu, J. (2011) 'Modeling stochastic live load for long-span bridge based on microscopic traffic flow simulation', *Computers and Structures*, Vol. 89, No. 9, pp. 813-824.

Chen, W., Ma, C., Xie, Z., Yan, B. and Xu, J. (2015) 'Improvement of extrapolation of traffic load effect on highway bridges based on Rice's theory', *International Journal of Steel Structures*, Vol. 15, No. 3, pp. 527-539.

Cremona, C. (2001) 'Optimal extrapolation of traffic load effects', *Structural Safety,* Vol. 23, No. 1, pp. 31-46.

Ditlevsen, O. (1994) 'Traffic loads on large bridges modeled as white-noise fields', *Journal of Engineering Mechanics*, Vol. 120, No. 4, pp. 681-694.

Enright, B. and OBrien E.J. (2013) 'Monte Carlo simulation of extreme traffic loading on short and medium span bridges', *Structure and Infrastructure Engineering*, Vol. 9, No. 12, pp. 1267-1282.

European Committee for Standardization (ECS). (2005) '*Eurocode 3: Design of steel structures: general rules and rules for buildings*', EN 1993–1-1, Brussels, Belgium.

Freire, A.M.S., Negrao, J.H.O. and Lopes, A.V. (2006). 'Geometrical nonlinearities on the static analysis of highly flexible steel cable-stayed bridges', *Computers and Structures,* Vol. 84, No. 31, pp. 2128-2140.

Fu, G. and You, J. (2009) 'Truck loads and bridge capacity evaluation in China', *Journal of Bridge Engineering*, Vol. 14, No. 5, pp. 327-335.

Han, W., Wu, J., Cai, C.S. and Chen, S. (2014) 'Characteristics and dynamic impact of overloaded extra heavy trucks on typical highway bridges', *Journal of Bridge Engineering*, Vol. 20, No. 2, pp. 05014011. (DOI: 10.1061/(ASCE)BE.1943-5592. 0000666).

Liu, Y., Deng, Y. and Cai, C.S. (2015) 'Deflection monitoring and assessment for a suspension bridge using a connected pipe system: a case study in China', *Structural Control and Health Monitoring*, Vol. 22, No. 12, pp. 1408-1425.

Lu, N., Noori, M. and Liu, Y. (2017a) 'Fatigue reliability assessment of welded steel bridge decks under stochastic truck loads via machine learning', *Journal of Bridge Engineering*, Vol. 22, No. 1, pp. 04016105. (DOI: 10.1061/(ASCE)BE.1943-5592.0000982)

Lu, N., Beer, M. and Liu Y. (2017b) 'Lifetime deflections of long-span bridges under dynamic and growing traffic loads', Journal of Bridge Engineering, Vol. 22, No. 11, pp. 04017086. (DOI: 10.1061/(ASCE)BE.1943-5592.0001125)

Miao, T.J. and Chan, T.H. (2002) 'Bridge live load models from WIM data', *Engineering structures*, Vol. 24, No. 8, pp. 1071-1084.

Ministry of Communications and Transportation (MOCAT) (2015). '*General code for design of highway bridges and culverts GB 60-2015*', Beijing, China. [In Chinese]

MOCAT, (2007). '*Specifications for design of highway cable-stayed bridge JTG/T D65-2007*', Beijing, China. [In Chinese].

Nowak A.S. (1994). Load model for bridge design code. *Canadian Journal of Civil Engineering*, Vol 21, No. 1, pp. 36-49.

OBrien, E.J. and Enright, B. (2012), 'Using weigh-in-motion data to determine aggressiveness of traffic for bridge loading'. *Journal of Bridge Engineering*, Vol. 18, No. 3, pp. 232-239.

OBrien, E.J., Bordallo-Ruiz, A. and Enright, B. (2014). Lifetime maximum load effects on short-span bridges subject to growing traffic volumes. *Structural Safety*, Vol. 50, pp. 113-122.

OBrien, E.J., Schmidt, F., Hajializadeh, D., Zhou, X., Enright, B., Caprani, C.C., Wilson, S. and Sheils, E. (2015) 'A review of probabilistic methods of assessment of load effects in bridges', *Structural Safety*, Vol. 53, No. 3, pp. 44-56.

Oconnor, A. and O'Brien, E.J. (2005) 'Traffic load modelling and factors influencing the accuracy of predicted extremes', *Canadian Journal of Civil Engineering*, Vol. 32, No. 1, pp. 270-278.

Rice, S. (1945) 'Mathematical analysis of random noise', *Bell System Technical Journal*, Vol. 24, No. 1, pp. 46-156.

Yu, Y., Cai, C.S. and Deng, L. (2016) 'State-of-the-art review on bridge weigh-in-motion technology', *Advances in Structural Engineering*, Vol. 19, No. 9, pp. 1514-1530.

Zhang, J. and Au, F.T.K. (2017) 'Fatigue reliability assessment considering traffic flow variation based on weigh-in-motion data', *Advances in Structural Engineering*. Vol. 20, No. 1, pp. 125-138.

Zhou, X.Y., Schmidt, F., Toutlemonde, F. and Jacob, B. (2016) 'A mixture peaks over threshold approach for predicting extreme bridge traffic load effects', *Probabilistic Engineering Mechanics* Vol. 43, pp. 121-131.

Table Captions

Table 1 Overview of WIM measurements
Table 2 Parameters of the level-crossing rates accounting for traffic densities

Table 1 Overview of WIM measurements

Items	Values
Time period	May 1, 2013 to April 30, 2015
Number of recording days	729
Average daily truck traffic	2145
Traffic lanes	4
Maximum GVW (t)	164

Table 2 Parameters of the level-crossing rates accounting for traffic densities

Traffic states	Sparse traffic	Moderate traffic	Dense traffic	Actual traffic
$v_{0,\mathrm{opt}}$	1274	751	675	859
m_{opt} (m)	0.2662	0.358	0.3352	0.249
σ_{opt} (m)	0.0427	0.0354	0.0746	0.0869

Figure captions

Figure 1 Principle of the level-crossing theory
Figure 2 Histograms of traffic volume in the same direction of a highway bridge
Figure 3 Flowchart of the computational framework
Figure 4 Statistics of the WIM measurements: (a) GVWs of 6-axle trucks; (b) vehicle spacing
Figure 5 Dimensions of a half of the cable-stayed bridge
Figure 6 Finite element model of the cable-stayed bridge
Figure 7 **Static deflection influence lines of the bridge girders at positions $L/4$, $L/2$ and $3L/4$**
Figure 8 Daily deflection history of the mid-span point of the bridge girder
Figure 9 Histograms and fittings of the number of level-crossings
Figure 10 Influence of the traffic proportion on the level-crossing rate
Figure 11 Maximum deflection of the bridge under traffic loads
Figure 12 Influence of traffic proportion on the maximum deflection extrapolation
Figure 13 Probability of exceedance of the threshold deflection
Figure 14 Influence of the reduction of the vehicle spacing on the probability of exceedance

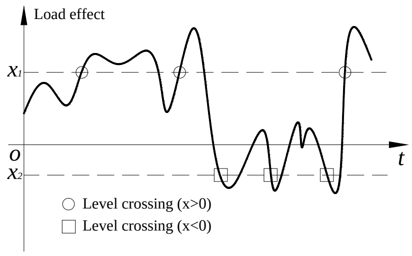

Figure 1 Principle of the level-crossing theory

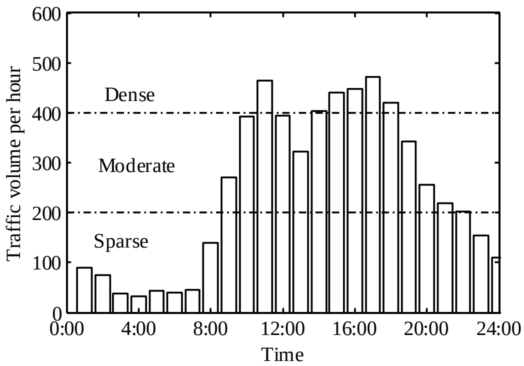

Figure 2 Histograms of traffic volume in the same direction of a highway bridge

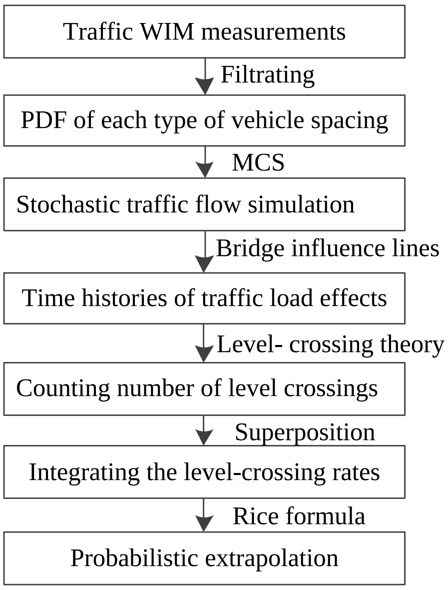

Figure 3 Flowchart of the computational framework

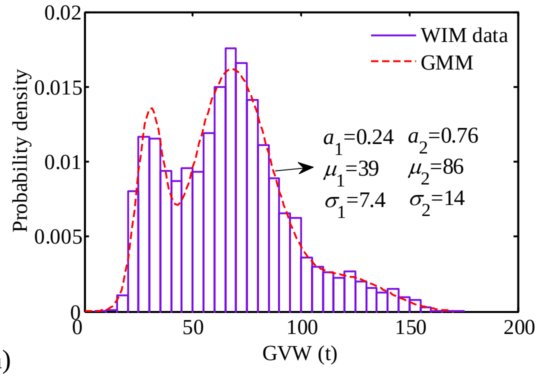

(a)

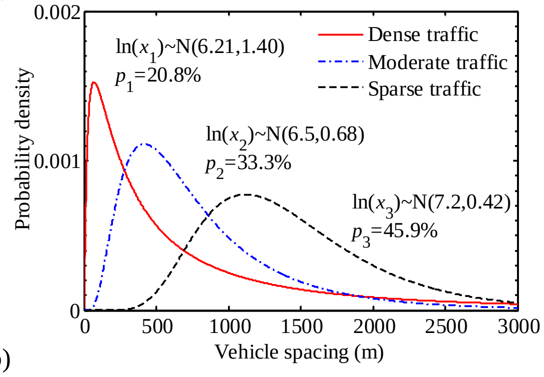

(b)

Figure 4 Statistics of the WIM measurements: (a) GVWs of 6-axle trucks; (b) vehicle spacing

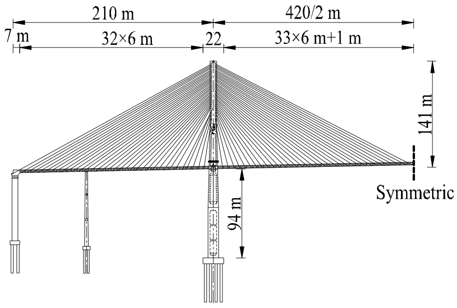

Figure 5 Dimensions of a half of the cable-stayed bridge

Figure 6 Finite element model of the cable-stayed bridge

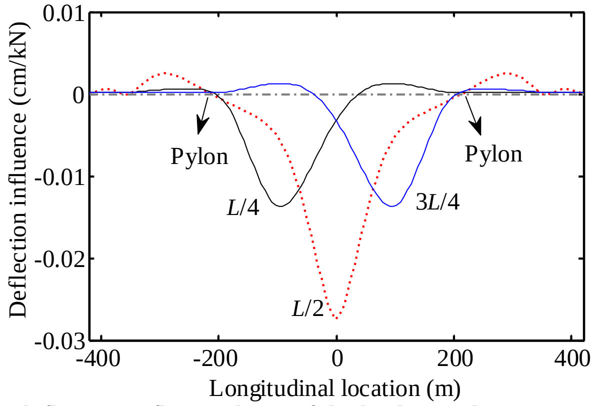

Figure 7 Static deflection influence lines of the bridge girders at positions $L/4$, $L/2$ and $3L/4$

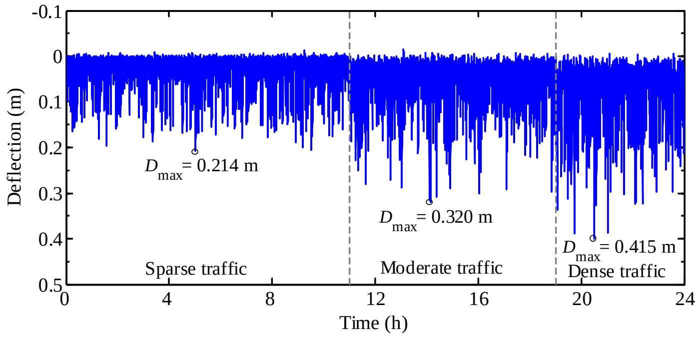

Figure 8 Daily deflection history of the mid-span point of the bridge girder

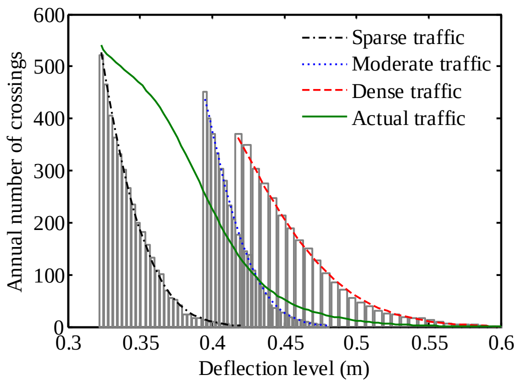

Figure 9 Histograms and fittings of the number of level-crossings

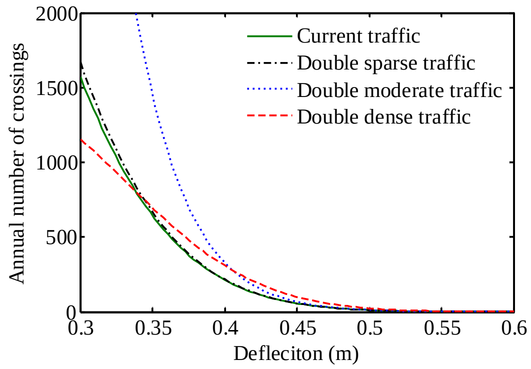

Figure 10 Influence of the traffic proportion on the level-crossing rate

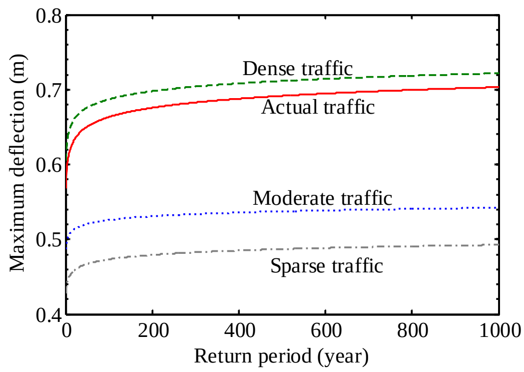

Figure 11 Maximum deflection of the bridge under traffic loads

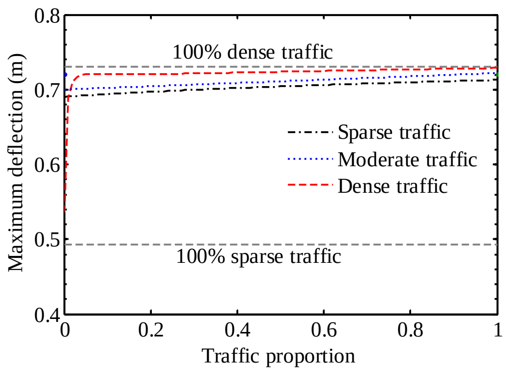

Figure 12 Influence of traffic proportion on the maximum deflection extrapolation

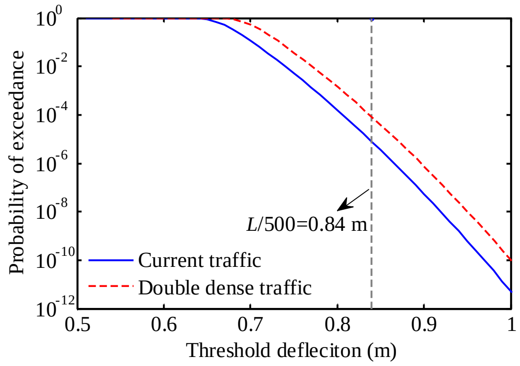

Figure 13 Probability of exceedance of the threshold deflection

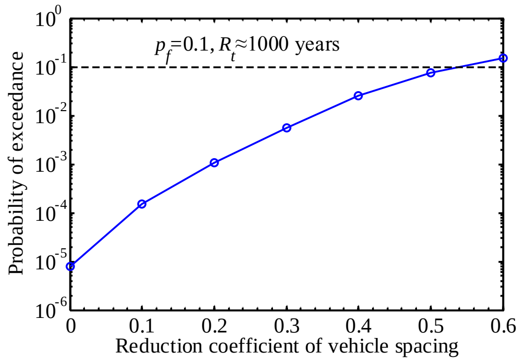

Figure 14 Influence of the reduction of the vehicle spacing on the probability of exceedance